Gait & Posture 40 (2014) 664–669

Contents lists available at ScienceDirect

Gait & Posture

journal homepage: www.elsevier.com/locate/gaitpost

A method to model anticipatory postural control in driver braking events

Jonas Östh [a,*], Erik Eliasson [a,1], Riender Happee [b,2], Karin Brolin [a,3]

[a] Chalmers University of Technology, Department of Applied Mechanics, Division of Vehicle Safety, Gothenburg, Sweden
[b] BioMechanical Engineering, Faculty of Mechanical, Maritime and Materials Engineering, Delft University of Technology, The Netherlands

ARTICLE INFO

Article history:
Received 23 January 2014
Received in revised form 17 July 2014
Accepted 22 July 2014

Keywords:
Human body model
Anticipatory postural control
Active muscles
Driver braking

ABSTRACT

Human body models (HBMs) for vehicle occupant simulations have recently been extended with active muscles and postural control strategies. Feedback control has been used to model occupant responses to autonomous braking interventions. However, driver postural responses during driver initiated braking differ greatly from autonomous braking. In the present study, an anticipatory postural response was hypothesized, modelled in a whole-body HBM with feedback controlled muscles, and validated using existing volunteer data. The anticipatory response was modelled as a time dependent change in the reference value for the feedback controllers, which generates correcting moments to counteract the braking deceleration. The results showed that, in 11 m/s^2 driver braking simulations, including the anticipatory postural response reduced the peak forward displacement of the head by 100 mm, of the shoulder by 30 mm, while the peak head flexion rotation was reduced by 18°. The HBM kinematic response was within a one standard deviation corridor of corresponding test data from volunteers performing maximum braking. It was concluded that the hypothesized anticipatory responses can be modelled by changing the reference positions of the individual joint feedback controllers that regulate muscle activation levels. The addition of anticipatory postural control muscle activations appears to explain the difference in occupant kinematics between driver and autonomous braking. This method of modelling postural reactions can be applied to the simulation of other driver voluntary actions, such as emergency avoidance by steering.

1. Introduction

Numerical human body models (HBMs) are used for research and development of vehicle occupant protection systems [1,2]. Recently, an interest in simulation not only of the crash phase, but also of the pre-crash phase, of road accidents has led to implementation of active muscles and control strategies in HBMs. Feedback control is suitable to model occupant postural responses in autonomous braking interventions [3,4]. In volunteer experiments, it was found that during driver initiated braking, drivers more effectively maintained their initial posture than during autonomous braking interventions [5,6]. For example, forward head displacements for males ($n = 11$) were 35 (SD 37) mm on average in driver braking; this is significantly less ($p < 0.05$) than the 98 (SD 65) mm found for autonomous braking of the same magnitude, 11 m/s^2 [5]. Driver initiated braking differs from autonomous braking in that the driver performs a voluntary action. The driver rapidly shifts his foot from the accelerator to the brake pedal, extends the hip and thigh, and plantarflexes the ankle with relatively high muscle efforts [7].

For other types of voluntary actions, anticipatory postural responses are found before activation of the prime movers [8–12]. For instance, prior to step initiation, anticipatory postural adjustments initiate a forward and lateral movement of the body mass [9]; during falling anticipatory muscle activity prepares the body for impact [10]; lifting of the arm while standing generates leg muscle activation 50–100 ms prior to activation of the prime

* Corresponding author at: Applied Mechanics, Vehicle Safety, Chalmers University of Technology, SE-412 96 Göteborg, Sweden. Tel.: +46 31 772 15 36.
E-mail addresses: jonas.osth@chalmers.se (J. Östh), erikeli@student.chalmers.se (E. Eliasson), R.Happee@tudelft.nl (R. Happee), karin.brolin@chalmers.se (K. Brolin).
[1] Address: Applied Mechanics, Vehicle Safety, Chalmers University of Technology, SE-412 96 Göteborg, Sweden.
[2] Address: Mekelweg 2, 2628CD, The Netherlands. Tel.: +31 152783213.
[3] Address: Applied Mechanics, Vehicle Safety, Chalmers University of Technology, SE-412 96 Göteborg, Sweden. Tel.: +46 31 772 15 09.

http://dx.doi.org/10.1016/j.gaitpost.2014.07.021

movers of the arm [11]. These anticipatory responses are generated by the central nervous system (CNS) in a feed-forward manner to generate approximate correcting muscle activations in various body parts prior to postural perturbations [12]. In the present study, a method to model anticipatory postural responses in HBMs for occupant simulation is investigated and applied to study maximum driver braking.

2. Methods

A whole body Finite Element (FE) HBM, the THUMS® AM50 v3.0 [2], was used in this study (Fig. 1). The model contains rigid bodies (e.g., the vertebrae) and deformable parts (e.g., the intervertebral discs, ribs, skin, and internal organs), totalling 68 100 solid elements, 75 700 shell elements, and 3400 one-dimensional elements. Some changes were made to the THUMS® for this study [4]. The hip joints were modelled with ball joints positioned in the femoral head [13]. As the current study included frontal loading only, the irrelevant hip degrees of freedom, abduction–adduction and medial–lateral rotation, were constrained by high passive stiffnesses (20 000 Nm/rad). The knee and ankle joints were modelled with revolute joints positioned according to [14,15], respectively. The FE solver LS-DYNA® version 971, release 6.1.0 (LSTC Inc., Livermore, CA, USA) was used. Pre- and post-processing were done with LS-PREPOST® v4.0 (LSTC Inc., Livermore, CA, USA) and MatLab® R2012b (The Mathworks Inc., Natick, MA, USA).

2.1. Musculoskeletal feedback control model

The THUMS® model has previously been complemented with 348 line muscle elements representing the muscles of the neck, lumbar and abdominal areas [4], and the upper extremities [16]. A Hill-type muscle material is used, in which the maximum isometric stress is 1 MPa for the upper extremity muscles [17] and 0.5 MPa [18] for the other muscles in the model. Two different values were chosen to give the model maximum isometric strengths of similar magnitude as that of volunteers. For example, in elbow flexion and extension, the model strength is 86 Nm and 48 Nm compared with volunteers 78 (SD 11) Nm and 50 (SD 11) Nm [19]. For cervical flexion and extension the model strength is 32 Nm and 48 Nm compared with volunteers 30 (SD 5) Nm and 40 (SD 8) Nm [5], measured relative to T1.

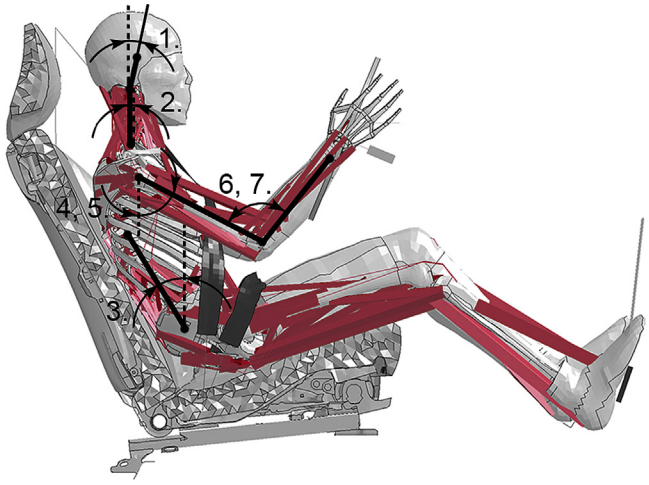

Fig. 1. The controller angles for the (1) head, (2) neck, (3) lumbar spine, (4) left and (5) right shoulder all use the angle of the body part with respect to the vertical axis. The (6) left and (7) right elbow controllers utilize the relative angle between the humerus and ulna. Soft tissues of the trunk, neck, and upper extremities and half the seat are not shown to disclose the musculoskeletal structure of the model.

To model postural control and response to external loads, seven proportional, integral, and derivative (PID) controllers were implemented. The control signals are defined as the angle in the sagittal plane between the vertical axis and a vector defined by two nodes in the model, and for the elbow controllers as the angle between vectors spanning the humeri, from the centre of the glenohumeral joint to the elbow, and ulnae, from the elbow joint to the distal end of the ulna (Fig. 1). The lumbar vector extends from the sacrum to the vertebral body of T10, the cervical vector from the vertebral body of T1 to the mid occipital condyles, and the head vector from the mid occipital condyles to the head centre of gravity. Head centre of gravity is determined according to the mass distribution of the models skull, flesh, and brain. The PID controllers are hypothesized to represent vestibular and proprioceptive feedback; they generate a control signal, $u(t)$, computed according to:

$$e(t) = r(t) - y(t - T_{de}) \tag{1}$$

$$u(t) = k_p * e(t) + k_i * \int_0^t e(\tau)d\tau + k_d * \frac{de(t)}{dt} \tag{2}$$

The joint angle, $y(t - T_{de})$, is compared with the reference, $r(t)$, and the control signal is proportional to the error, $e(t)$, between the two, Eq. (2), with proportional feedback gain, k_p, integrative feedback gain, k_i, and differential (velocity) feedback gain, k_d. The proportional and velocity gains can be considered as generic representations of reflexes responsible for the maintenance of posture, i.e. muscle spindle feedback [20] and vestibular reflexive stabilization [21], while the integrative controller corrects any residual error and maintains the desired posture in the presence of gravity. The transport delay, T_{de}, accounts for the time needed for the neural signal to be conveyed to and from the CNS. T_{de} was 34 ms for the elbow and 30 ms for the shoulder [22] controller. For the head and neck T_{de} was 20 ms, i.e. a shorter delay was estimated due to the proximity to the spinal cord, matching the 18 ms delay reported for the cervicocollic reflex in cats [21]. For the lumbar controller, T_{de} was 25 ms, which is relatively close to the 30 ms that has been reported for the lumbar spine muscles [23]. The control signal, $u(t)$, is converted to a muscle activation request by scaling with the maximum isometric strength of each controlled muscle group. The scaled activation request is passed through a muscle excitation–contraction dynamics model consisting of two coupled first order filters [24], giving a muscle activation level, $N_a(t)$. A generic muscle recruitment strategy divides the muscles of each controlled joint into either flexors or extensors, with the same activation level. Co-contraction of muscles around the controlled joints is implemented as a lower bound on the muscle activation, i.e. all muscles always have a prescribed minimum activation level as selected below.

2.2. Lower extremity muscle implementation

For the lower extremities, Hill-type line muscles were added, see Table 1. To account for the curvature of the gluteus maximus around the pelvis and of the quadriceps and patellar tendons over the knee, the Hill-elements were coupled in series with stiff (10 000 N/engineering strain) "seat belt" elements. These elements were fed through slip rings attached to the pelvis for the gluteus maximus and to the distal head of the femur and proximal head of the tibia for the quadriceps and patellar tendon.

2.3. Maximum driver braking simulations

Volunteer kinematics, interaction forces, and muscle contraction levels in 11 m/s^2 driver braking events from 70 km/h to a

Table 1
Lower extremity muscles in the HBM. Muscle origin and insertions point taken from the anatomical descriptions of [25]. The physiological cross sectional areas (PCSAs) are from [26]. Actions of the muscles in the model: HF – hip flexion; HE – hip extension; KF – knee flexion; KE – knee extension; PF – plantar flexion; DF – dorsiflexion. NEL – number of elements. Muscle data for the upper body and extremities are presented in [4,16].

Muscle	NEL	Origin	Insertion	PCSA (mm^2)	Action	Activation[a]
Adductor longus	1	Front of pubis	Linea aspera, mid femur	650	HF	0.26
Adductor magnus	4	Inferior ramus of pubis	Linea aspera, along femur	2130	HE	0.54
Biceps femoris	2	Ischial tuberosity and linea aspera, mid femur	Lateral condyle of tibia	1680	HE, KF	0.26
Gastrocnemius	2	Medial and lateral condyles of femur	Calcaneal tuberosity	3130	KF, PF	0.43
Gluteus maximus	3	Iliac crest and coccyx	Gluteal tuberosity on femur	3040	HE	0.54
Iliacus	1	Iliac fossa	Lesser trochanter	1020	HF	0.26
Pectineus	1	Pectineal line	Linea aspera, proximal end	290	HF	0.26
Psoas	1	L2 vertebra	Lesser trochanter	790	HF	0.26
Rectus femoris	1	Anterior inferior iliac spine	Quadriceps tendon	1390	HF, KE	0.57
Sartorius	1	Anterior superior iliac spine	Proximal, medial surface of tibia	190	HF, KF	0.26
Semi-membranosus	1	Ischial tuberosity	Medial tibial condyle	1910	HE, KF	0.26
Semitendinosus	1	Ischial tuberosity	Proximal, medial surface of tibia	490	HE, KF	0.26
Tibialis anterior	1	Proximal, lateral side of tibia	Medial cuneiform	1100	DF	0.18
Vastus	3	Anterior, upper third of femur	Quadriceps tendon	7750	KE	0.54

[a] Activation levels selected in simulations of voluntary braking based on normalized electromyogram (EMG) data from volunteers in emergency braking events reported by Behr et al. [7].

complete stop were reported by Östh et al. [5]. In the present study, data from eleven male subjects, average height of 178 (SD 5) cm and weight of 78 (SD 6) kg, was used for comparison with the HBM response. The HBM was positioned in an FE model of the test vehicle seat (Fig. 1) with a standard automotive three-point seat belt, passing over the pelvis, chest, and left shoulder of the model. Belt force was measured in the top shoulder belt mount. The hands of the HBM were attached to a simplified steering wheel, and compressive force in the steering column was recorded. The brake pedal was modelled according to its geometry in the test vehicle and translated 50 mm to place it symmetrically under the right foot of the HBM. The deceleration load was applied to the seat. To simulate voluntary braking, pressing the brake pedal with the right leg was modelled by open loop control by application of constant muscle activation levels after $t = 0$ s, Table 1, taken from the maximum effort normalized electromyogram (EMG) data in emergency braking events reported by Behr et al. [7]. The left leg muscles were activated with 6% of the activations for the right leg to provide foot rest interaction forces of the same magnitude as in the volunteer tests.

Three postural control strategies were evaluated. First, REF, a reflexive baseline strategy using controller gains and co-contraction levels, previously validated for 11 m/s^2 autonomous braking events [16]. In this baseline strategy, all reference signals, $r(t)$, were

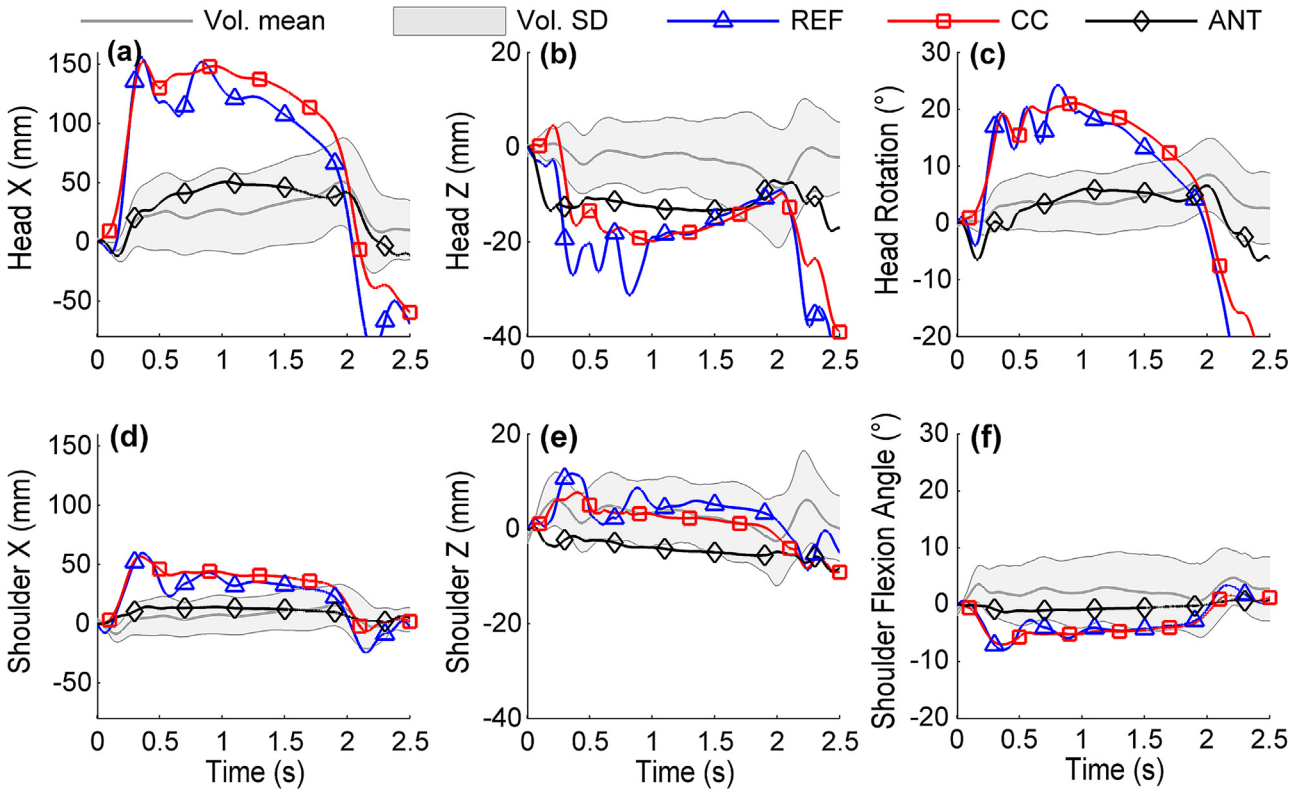

Fig. 2. Head centre of gravity and shoulder kinematics, evaluated at the centre of the right glenohumeral joint, for the HBM: REF – base line with reflexive control only; CC – co-contraction added; ANT – anticipatory control added. These are compared with the mean volunteer (Vol.) response ± 1 standard deviation (SD) from [5]. The head rotation angle, (c) and (f), corresponds to the head controller angle.

constant equal to zero; hence, postural feedback control was aiming to maintain the initial posture. Proportional gains of 6 Nm/rad, 12 Nm/rad, 88 Nm/rad, 54 Nm/rad, and 97 Nm/rad were used for the head, neck, lumbar, shoulder, and elbow controllers respectively. The differential gains were 4 Nms/rad, 4 Nms/rad, 12 Nms/rad, 22 Nms/rad, and 3 Nms/rad, while integral gains were 8 Nm/rads, 14 Nm/rads, 0 Nm/rads, 51 Nm/rads, and 48 Nm/rads, for each controller (in the same order). Furthermore, for all muscles an initial co-contraction level as a percentage of full muscular activation was estimated; in the REF strategy the head, cervical, and lumbar muscles had a co-contraction of 3% and the upper extremity muscles 4%, based on the range found for volunteers during quiet driving [5].

Second, CC, in which the average peak initial co-contraction found in the volunteer data [5] was applied as constant for the whole event (head and neck 11%, lumbar 6.5%, elbow 14%, and shoulder 21%) together with the baseline (REF) controller gains.

Third, ANT, in which the hypothesized anticipatory postural response was applied together with the reflexive gains and co-contractions used in CC. This was modelled with a time dependent reference value in the PID controllers, $r(t)$, which is proportional to the vehicle acceleration pulse but advanced 0.05 s, to make the onset timing of the anticipatory muscle response similar to those reported experimentally [11]. At 11 m/s^2 deceleration, the reference for the head controller was 0.15 rad extension from the initial position, for the neck 0.46 rad, the lumbar spine 0.64 rad, and the elbows 0.09 rad. For example, for the neck controller, a proportionality constant of 0.042 rad/m/s^2 (i.e. 0.46 rad/11 m/s^2) was used. These values were chosen so the model generated correcting moments of the same magnitude as the volunteers, calculated from normalized EMG and maximum voluntary strength. Furthermore, the integral gains for the head and neck controllers were half of that in the baseline strategy (REF).

3. Results

Resulting kinematics, interaction forces, and muscle activation levels for the HBM simulations are shown in Figs. 2–4, with the volunteer corridors. With the base line control strategy (REF), the simulated forward displacements, measured for the head centre of gravity and the centre of the right glenohumeral joint (Fig. 2(a and d)), head rotation (Fig. 2(c)), and shoulder flexion angles (Fig. 2(f)) were too large compared with the volunteer corridor. Increasing the co-contractions (CC) reduced the oscillations, but not the magnitude of the kinematic responses. For the anticipatory control strategy (ANT), the model is inside the volunteer kinematic corridors for most of the events, except for the head and shoulder Z displacements (Fig. 2(b and e)). During steady state braking, in the 1.5–1.7 s interval, the average head X displacement for the base line strategy (REF) was 99 mm, with increased co-contraction (CC) it was 121 mm, and with the anticipatory control strategy (ANT) 44 mm. The base line (REF) and co-contraction (CC) head kinematics are of similar magnitude as head X displacements of 98 (SD 65) mm for volunteers in autonomous braking [5], while the anticipatory control strategy (ANT) is more similar to the 35 (SD 37) mm for braking drivers [5].

The main difference between the control strategies with respect to the interaction forces (Fig. 3), was that for the anticipatory control (ANT) there is no initial peak in shoulder belt force, as found for the other two controller strategies, 71 N (REF) and 65 N (CC). With the prescribed constant muscle activations for the lower extremities, the model generated a brake pedal force of 380 N in all simulations.

With the anticipatory control (ANT), a rapid increase in lumbar extensor activation was seen shortly after $t = 0$ s, because the reference for the lumbar controller was changed (Fig. 4(b)). A similar increase was seen for the cervical extensors, but the difference, when compared with REF and CC, was not as apparent. For the elbow extensors and shoulder flexors (Fig. 4(c and d)) the largest activation was found for the baseline (REF) strategy. For the antagonistic muscles (Fig. 4(e and h)) constant co-contraction activations as prescribed were found for all control strategies.

4. Discussion

A novel method to model anticipatory postural responses in car occupant models during driver braking was presented. It is implemented using a PID-feedback control algorithm that employs joint angles to generate correcting muscle activations. The reference signal for the PID-controllers is changed so that the error, relative to the initial position, multiplied by the proportional gain of the controller, generates a restoring moment of the same magnitude as can be derived from maximum voluntary contraction normalized EMG recordings in the corresponding volunteer tests (approx. 1 Nm for the head, 3.5 Nm for the neck, 56 Nm for the lumbar, 9 Nm for the elbow). The reference signal was advanced in time relative to the acceleration pulse, which mainly influences the initial response of the model. For the shoulder a constant reference equal to the initial position was used, since a limited net moment was found in the volunteer data [5]. For the anticipatory control simulations, the integral gains of the head and neck were reduced, because the integrated error half-way through the simulation generates an extension moment that is too large.

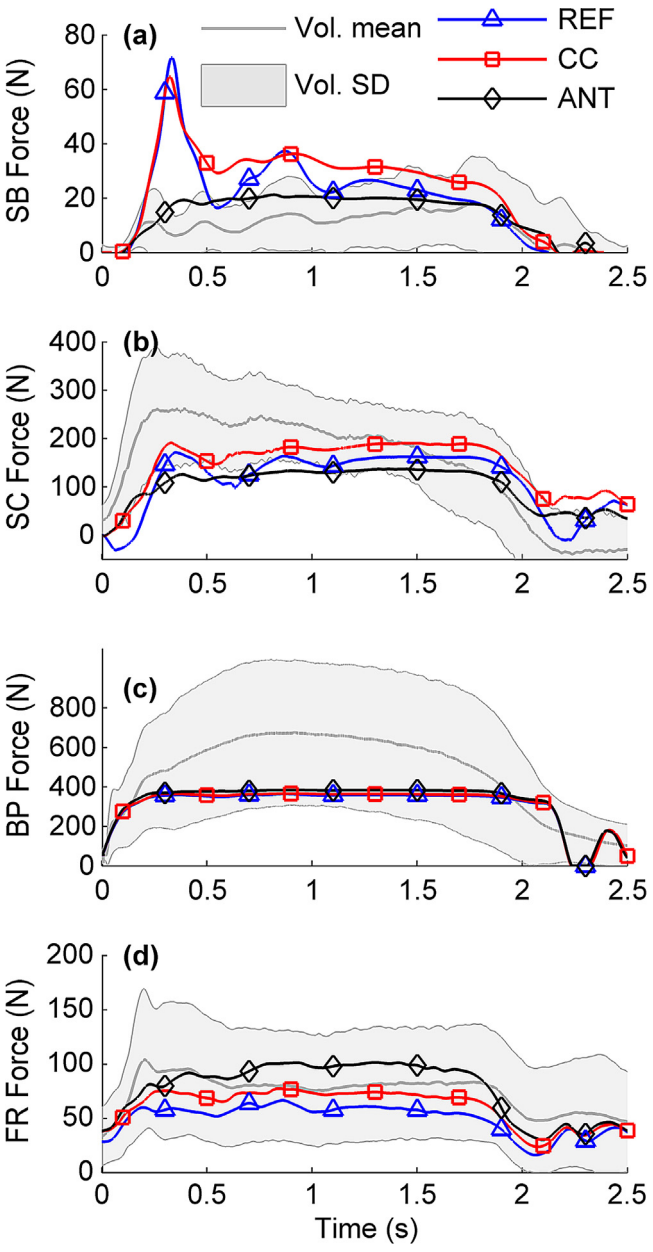

Fig. 3. The forces shown here are SB – shoulder belt, SC – steering column, BP – brake pedal, and FR – foot rest for the HBM with the REF – base line, CC – co-contraction, and ANT – anticipatory control strategies. These are compared with the Vol. = mean volunteer response ± 1 standard deviation (SD) from [5].

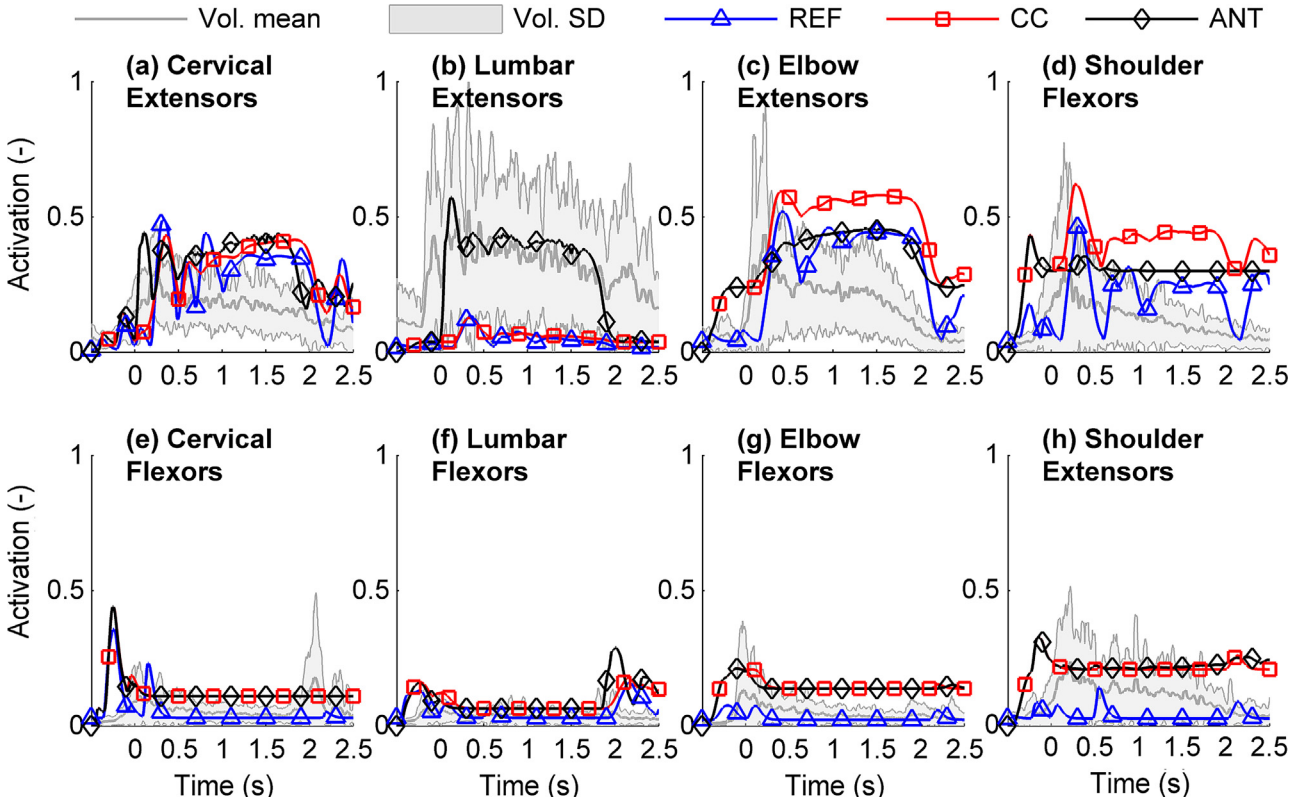

Fig. 4. Muscle activation levels for the HBM with REF – base line, CC – co-contraction, and ANT – anticipatory control strategies, compared with the mean maximum voluntary contraction normalized EMG of Vol. = volunteers ± 1 standard deviation (SD) in driver maximum braking tests [5].

As the anticipatory response is proportional to the braking deceleration simulated, the model has the potential to predict other driver braking scenarios. It was also noticed that higher co-contraction levels, as evaluated with the CC postural control strategy, provided a more damped kinematic HBM response than the baseline strategy but did not improve the prediction of the postural response of braking drivers.

The current HBM has "joint" sensors at the neck, lumbar spine, shoulder and elbows, and a spatial orientation sensor for the head (Fig. 1). The vestibular organs sense head motion in space, but certainly no joint sensors like those in the model exist in other body parts. However, the integrated visual, vestibular, and somatosensory information most certainly provide joint angle information; as stated by Winter [8], the CNS is "...totally aware of the problems of controlling a multisegment system" (p. 194), in the motivation to use an inverted pendulum to model quiet standing.

The anticipatory control is based on the scaled acceleration curve, with the assumption that the CNS can predict the upcoming acceleration, resulting from driver initiated braking. All drivers in the volunteer study [5] that provided the validation data for the HBM were experienced drivers. They have performed driver braking frequently at varying deceleration levels. Hence, it is reasonable that their CNS expects the coming perturbation and provides an effective anticipatory postural response. Drivers performing emergency braking in a fixed base vehicle simulator [27], braced by moving rearward into the seat and extended their arms and legs. This motion is the same as the change of reference for the PID-controllers will impose, but here and in the volunteer test counterpart it is counteracted by the acceleration of the braking car.

In the present study, the inclusion of an anticipatory postural response was able to capture the postural response of car drivers in voluntary braking, while previously feedback control has sufficed for autonomous interventions [3,4]. Collision mitigation systems that aim to protect vehicle occupants by autonomous braking are often combined with auditory and visual alerts [28]. Such warnings, or the activation of a pre-tensioned seat belt [5], might cause a startle response [29], i.e. a short simultaneous contraction of all muscles. The combination of feedback control, anticipatory control, and startle responses in combined braking scenarios remains to be investigated. However, the model presented can also represent startle responses by the inclusion of open loop muscle activation impulses, for example through an impulse change of the prescribed co-contraction levels.

To conclude, driver anticipatory postural responses during driver braking were modelled in an HBM through changes of the reference positions for feedback controllers that regulate muscle activation levels. The addition of anticipatory postural control muscle activations could explain the difference in occupant kinematics between driver and autonomous braking. This method of modelling postural reactions should have application for simulation of other driver voluntary actions, such as emergency avoidance by steering.

Acknowledgements

This study was carried out at SAFER, the Vehicle and Traffic Safety Centre, at Chalmers, Gothenburg, Sweden. It was funded by VINNOVA, the Swedish Governmental Agency for Innovation Systems, as part of the FFI Vehicle and Traffic Safety research programme. Project partners were Autoliv Research AB, Volvo Group, Volvo Car Corporation, and Umeå University. The authors would like to thank Niklas Blomgren, Joakim Ericson, and Oscar Lundahl, for contributions in generating the lower extremity model, and Lora Sharp McQueen for language editing of the manuscript.

Conflict of interest statement

The authors have no conflicts of interest.

References

[1] Happee R, Hoofman M, van den Kroonenberg AJ, Morsink P, Wismans J. A mathematical human body model for frontal and rearward seated automotive impact loading. In: Proceedings of the 42nd Stapp Car Crash Conference; 1998. p. 75–88.

[2] Iwamoto M, Kisanuki Y, Watanabe I, Furusu K, Miki K. Development of a finite element model of the Total HUman Model for Safety (THUMS) and application to injury reconstruction. In: Proceedings of the IRCOBI Conference; 2002.

[3] Meijer R, van Hassel E, Broos J, Elrofai H, van Rooij L, van Hooijdonk P. Development of a multi-body human model that predicts active and passive human behaviour. In: Proceedings of the IRCOBI Conference; 2012.

[4] Östh J, Brolin K, Carlsson S, Davidsson J, Wismans J. The occupant response to autonomous braking: a modeling approach that accounts for active musculature. Traffic Inj Prev 2012;13:265–77.

[5] Östh J, Ólafsdóttir JM, Davidsson J, Brolin K. Driver kinematic and muscle responses in braking events with standard and reversible pre-tensioned restraints: validation data for human models. Stapp Car Crash J 2013;57:1–41.

[6] van Rooij L, Pauwelussen J, Op den Camp O, Janssen R. Driver head displacement during (automatic) vehicle braking tests with varying levels of distraction. In: Proceedings of the 23rd ESV Conference; 2013.

[7] Behr M, Poumarat G, Serre T, Arnoux P-J, Thollon L, Brunet C. Posture and muscular behavior in emergency braking: an experimental approach. Accid Anal Prev 2010;42:797–801.

[8] Winter DA. Human balance and posture control during standing and walking. Gait Posture 1995;3:193–214.

[9] MacKinnon CD, Bissig D, Chiusano J, Miller E, Rudnick L, Jager C, et al. Preparation of anticipatory postural adjustments prior to stepping. J Neurophysiol 2007;97:4368–79.

[10] Santello M. Review of motor control mechanisms underlying impact absorption from falls. Gait Posture 2005;21:85–94.

[11] Massion J. Movement, posture and equilibrium: interaction and coordination. Prog Neurobiol 1992;38:35–56.

[12] de Wolf S, Slijper H, Latash ML. Anticipatory postural adjustments during self-paced and reaction-time movements. Exp Brain Res 1998;121:7–19.

[13] Schofer MD, Pressel T, Heyse TJ, Schmitt J, Boudriot U. Radiological determination of the anatomic hip centre from pelvic landmarks. Acta Orthop Belg 2010;76:479–85.

[14] Frankel VH, Burstein AH, Brooks DB. Biomechanics of internal derangement of the knee: pathomechanics as determined by analysis of the instance centers of motion. J Bone Joint Surg Am 1971;53A:945–62.

[15] Baxter JR, Novack TA, van Werkhoven H, Pennell DR, Piazza SJ. Ankle joint mechanics and foot proportions differ between human sprinters and non-sprinters. Proc R Soc B 2012;279:2018–24.

[16] Östh J, Brolin K, Bråse D. A human body model with active muscles for simulation of pre-tensioned restraints in autonomous braking interventions. Traffic Inj Prev 2014. http://dx.doi.org/10.1080/15389588.2014.931949 [in press].

[17] An KN, Kaufman KR, Chao EYS. Physiological considerations of muscle force through the elbow joint. J Biomech 1989;22:1249–56.

[18] Hedenstierna S. 3D finite element modeling of cervical musculature and its effect on neck injury prevention.[PhD thesis] Stockholm, Sweden: Royal Institute of Technology; 2008.

[19] Buchanan TS, Delp SL, Solbeck JA. Muscular resistance to varus and valgus loads at the elbow. J Biomech Eng 1998;120:634–9.

[20] Mileusnic MP, Brown IE, Lan N, Loeb G. Mathematical models of proprioceptors. I. Control and transduction in the muscle spindle. J Neurophys 2006;96:1772–1780.

[21] Peterson BW, Goldberg J, Bilotto G, Fuller JH. Cervicocollic reflex: its dynamic properties and interaction with vestibular reflexes. J Neurophys 1985;54:90–109.

[22] de Vlugt E, Schouten AC, van der Helm FCT. Quantification of intrinsic and reflexive properties during multijoint arm posture. J Neurosci Methods 2006;155:328–49.

[23] van Drunen P, Maaswinkel E, van der Helm FCT, van Dieën JH, Happee R. Corrigendum to "Identifying intrinsic and reflexive contributions to low-back stabilization" [J. Biomech. 46(8) (2013) 1440–1446]. J Biomech 2014. http://dx.doi.org/10.1016/j.jbiomech.2014.03.013.

[24] Winters JM, Stark L. Analysis of fundamental human movement patterns through the use of in-depth antagonistic muscle models. IEEE Trans Biomed Eng 1985;32:826–39.

[25] Standring S, editor. Gray's anatomy – the anatomical basis of clinical practice. London, UK: Elsevier Churchill Livingstone; 2008.

[26] Arnold EM, Ward SR, Lieber RL, Delp SL. A model of the lower limb for analysis of human movement. Ann Biomed Eng 2010;38:269–79.

[27] Hault-Dubrulle A, Robach F, Pacaux M-P, Morvan H. Determination of pre-impact occupant postures and analysis of consequences on injury outcome. Part I: A driving simulator study. Accid Anal Prev 2011;43:66–74.

[28] Coelingh E, Jakobsson L, Lind H, Lindman M. Collision warning with auto brake – a real-life safety perspective. In: Proceedings of the 20th ESV Conference; 2007.

[29] Yeomans JS, Li L, Scott BW, Frankland PW. Tactile, acoustic and vestibular systems sum to elicit the startle reflex. Neurosci Biobehav Res 2002;26:1–11.